Petrophysical analysis for hydrocarbon exploration based on well log data, North Maryut, Mediterranean Sea, Egypt

Adel A.A Othman1, Tharwat, A.H.1, M.Fathy.[1], and Adel, M. Negm[2]

Geology Department, Faculty of Science, Al-Azhar University, Cairo, Egypt
adelnegm_88@yahoo.com

Abstract: Well logging is a study of acquiring information on physical properties of rocks that are exposed during drilling of an oil well. The key purpose of well logging is to obtain Petrophysical properties of reservoirs such as Porosity, hydrocarbon saturation etc., for hydrocarbon exploration. Petrophysical parameters such as effective porosity (Φ), water saturation (S_w), formation water resistivity (R_w), hydrocarbon saturation (S_{hr}) and true resistivity (R_t) are evaluated by using the well log data. This paper presents the log analysis results from two wells located in off shore Egypt in the western side of the Nile delta in water depth reach to 450m. The first well (North Idkue -4x) was drilled on Viper and Anaconda channel in lower Pliocene prospect to assess the reservoir presence, quality and commercial hydrocarbon potential of stacked, structurally and stratigraphically controlled Pliocene channel levee complex with seismic attributes anomalies while the second well(Raven -2) drilled on two channel (lower and upper channel) in lower Miocene.

[Adel A.A Othman, Tharwat, A.H, M. Fathy and Adel, M. Negm. **Petrophysical analysis for hydrocarbon exploration based on well log data, North Maryut, Mediterranean Sea, Egypt.** *J Am Sci* 2014;10(12):58-68]. (ISSN: 1545-1003). http://www.jofamericanscience.org. 6

Keyword: Petrophysical analysis**,** Well logging, seismic attributes, channel, N. Maryut

1. Introduction:

The general purpose of well log analysis is to convert the raw log data into estimated quantities of oil, gas and water in a formation (Asquith and Krygowski, 2004) Around 58 Tcf of gas reserves have been discovered until now in the Nile Delta province (Nini, 2010), it is therefore considered the most prolific province for gas production in Egypt. So, many international companies working hard in this province, a vast bibliography is available about the Nile Delta Basin regarding lithostratigraphy, depositional history, tectonic evolution, petroleum system, hydrocarbon characterization, among the many authors we can remember; Rizzini (1978), Said (1981 and 1990), Abdel Aal (2000), Dolson (2000), Tawadros (2001), Hemdan (2008) and Nini (2010). The study area located in the North western offshore part of the Mediterranean Sea, Egypt.it lies 50km north of Alexandria, between Abu Qir and Rosetta fields. The study area lies between latitude 31° 44′ 24.605″ – 31° 42′ 53.03″ N and longitude 29° 51′ 10.531″ – 30° 50′ 31.2″ E

2. Geologic setting:

The whole surface of the Nile Delta region is almost covered by recent sediments (silt and clay), of a thickness reaching about few tens of feet. Therefore, the stratigraphy and structure of the area are mainly concealed under these surface sediments except some few outcropping areas. The oldest unites that crop out in the Nile Delta region at Abu Roash dome, west of Cairo, belongs to the cretaceous, However, older stratigraphic units have been generally encountered in several wells. Regionally, the sedimentary succession is characterized by a sequence of Mesozoic and lower Eocene carbonates overlain by a northward thickening middle-late Eocene to Holocene mainly clastic deposits. The oldest sedimentary rocks penetrated in the Nile Delta are of Jurassic age. According to the generalized stratigraphic column of the Nile Delta area, as shown in (Figure 2), the sedimentary section of the Nile Delta ranges in age from Jurassic to Recent, where Jurassic section is resets unconformably on the basement.

The structural pattern of the offshore Nile Delta is the result of a complex interplay among three main fault trends. The NW-SE Misfaq-Bardawil (Temsah) fault trend, the NE-SW Qattara-Eratosthenes (Rosetta) fault trend and the E-W fault trend (Figure 3). These trends parallel the circum-Mediterranean plate boundaries, and seem to be old inherited basement faults that reactivate periodically throughout the development of the area. The Temsah and Rosetta oblique-slip faults intersect in the southern part of deep water block, creating a faulted, regional high. West of this high, the platform area forms an extension of the relatively unstructured Nile Delta province to the south (Abd El Aal, 2000).

Meshref (1982); Deduced that the northern Egypt including Nile Delta seems to be affected by the following three main tectonic events:

a) The oldest (Paleozoic-Tertiary) that produced N-W trending faults.

b) The second event (Cretaceous) that produced N-E (Syrian Arc) trending structures.

c) The third tectonics event (Late Eocene-Early Oligocene) that produced E-W, NNW (Suez) and NNE (Aqaba) trending structures.

In the study area this is not as thick as in the salt provinces to the north-west and in the Eastern Nile Delta, where it forms a significant decollement surface with associated fault block rotation and minor salt diapirism, setting up much of the trapping mechanisms.

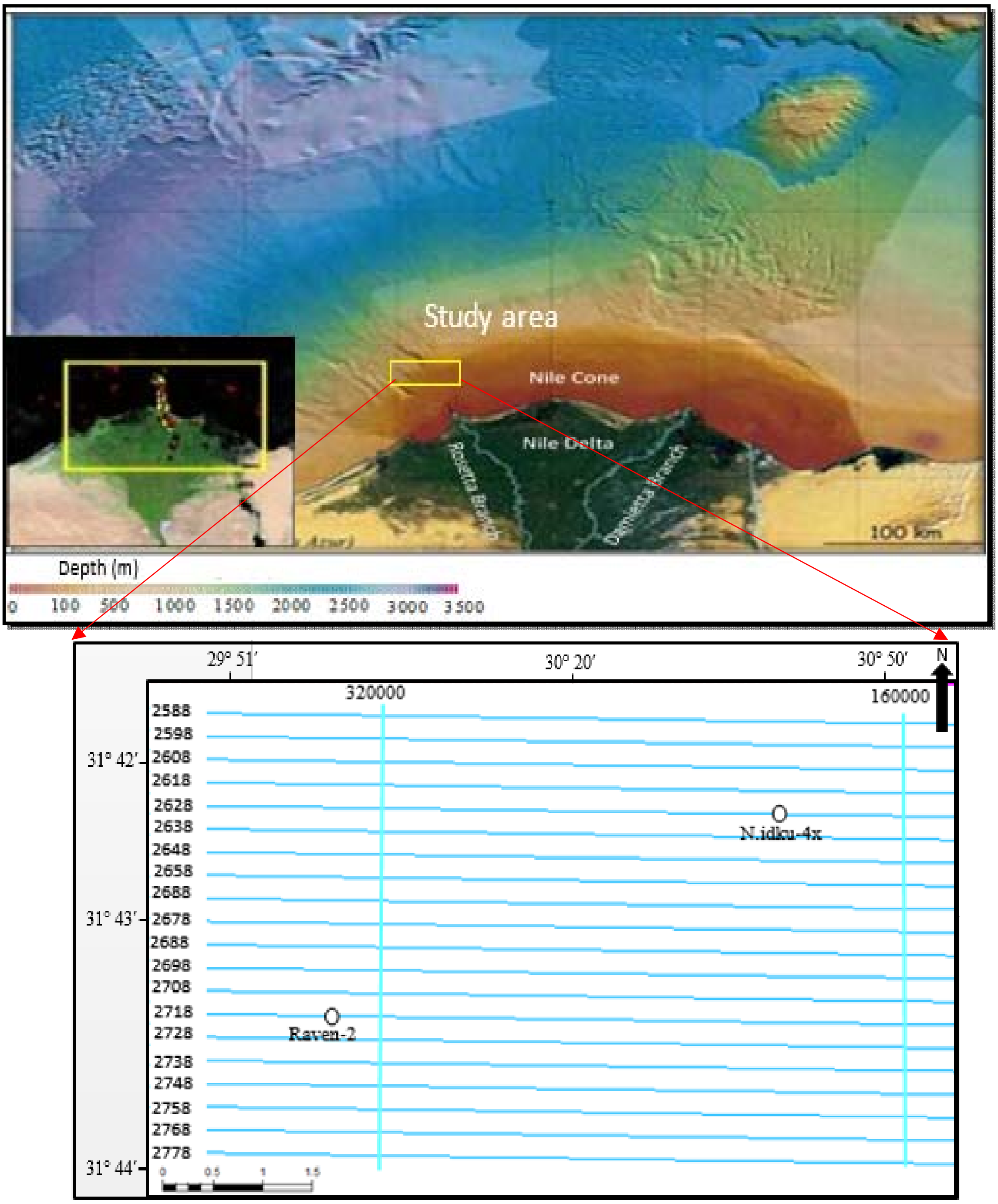

Figure (1): Location map of the study area showing the used well and seismic lines.

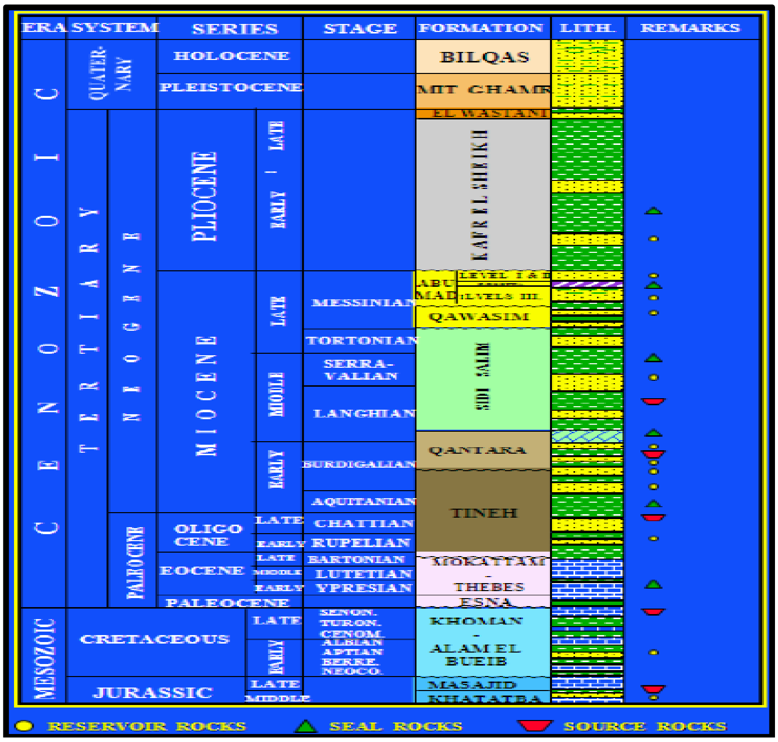

Figure (2): Generalized stratigraphic column of the Nile Delta (After ENI, 2000).

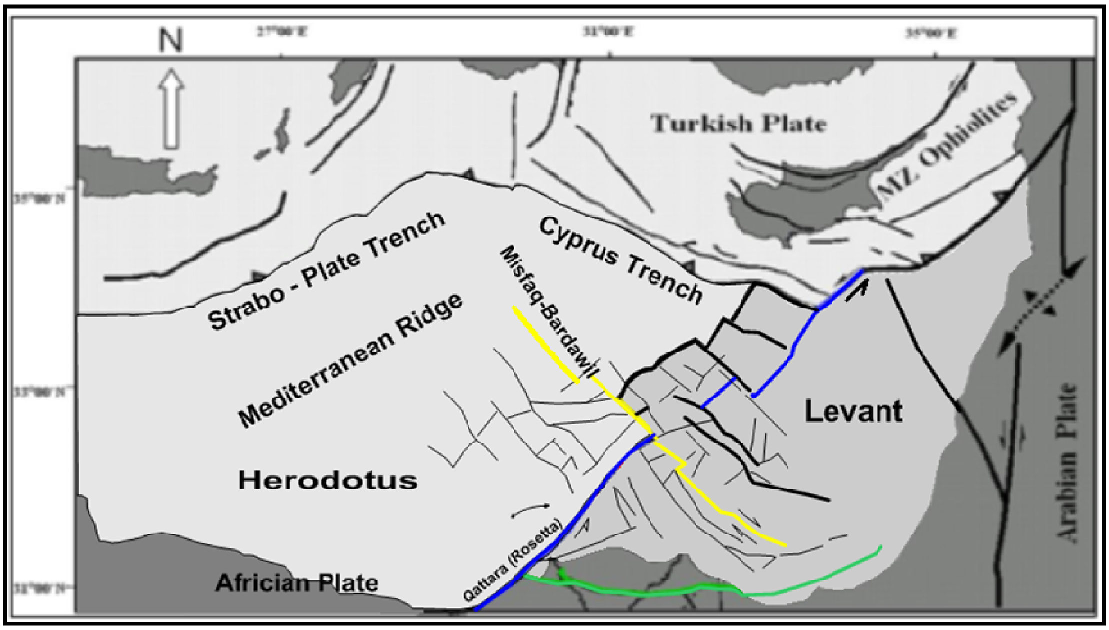

Figure (3): East Mediterranean structural domain with its main fault trends modified After (Abd El Aal, 2000).

Figure (4) showing the structural framework shows a series of faulted basement and pre-rift fault blocks with a Cretaceous hinge line over which the current delta and Paleo- Nile delta has prograded, resulting in a stacked pay system of slope channel deposits from Eocene to Recent. The pink Messinian horizon represents the salinity crisis, a time of extreme lowstand when the delta was exposed and deposition was dominated by anhydrites and halites.

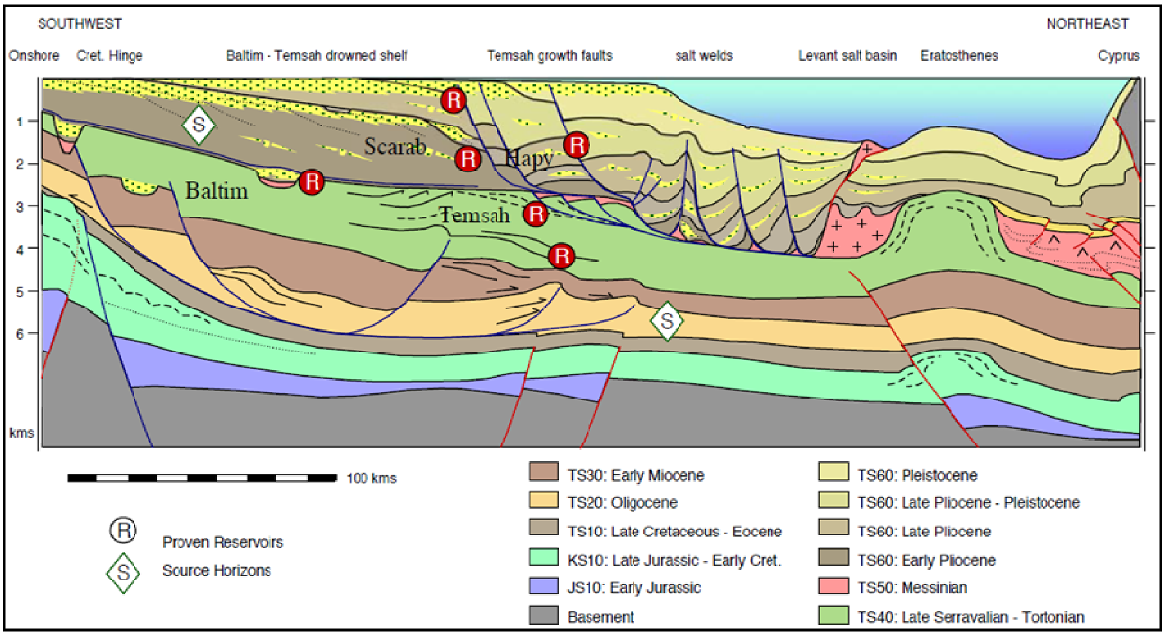

Figure (4): Schematic cross-section based on regional seismic profiles across the Nile Delta and Mediterranean showing major Petroleum plays. Most current activity targets the higher seismic data quality Pliocene and Messinian section, but deeper potential exists throughout the basin. (Dolson, 2000).

3. Methodology:

In the present study different wireline logging suites (Gamma ray, neutron, density, sonic, resistivity, etc.) are used in the analysis and performing the necessary calculations. The most important petrophysical parameters necessary for characterizing the potential reservoirs are deduced like, porosity (total and effective), shale volume, fluid saturation (water and hydrocarbon).and Utilizing of different techniques of Seismic attributes for tracking the channels boundaries by means of RMS amplitude and Relative acoustic impedance.

4. Results and Discussion:

4.1. Shale volume estimation:

Gamma ray electric log data is routinely used to compute shale volume. Equation 1 demonstrates the relationship to estimate shale volume from the gamma ray log. A weighting factor of 0.5 was applied to the gamma ray computed shale volume.

$$VSHgr = \frac{GR - GRmin}{GRmax - GRmin} \quad (1)$$

Where VSHgr-Shale volume gamma ray derived, GR- Gamma Ray Log value (API) and GRmin-Gamma Ray value of zero shale interval

For Raven -2 well, GRmin = 10 API and GRmax = 63 API while the North Idkue -4 well GRmin=38 API and GRmax =68 API

4.2. Porosity (PHI) AND Effective Porosity (PHIE_D) Calculations:

The formation porosity is very important for calculation the fluid saturation

The effective porosity calculations have been calculated for the two Wells by using density, shale volume logs and the following equations (Schlumberger, 1972). Table (5.2) shows the used parameters in calculating effective porosity for all intervals for the studied two wells

$$\Phi_T = [\rho_{ma} - \rho_B] / [\rho_{ma} - \rho_f] \quad (2)$$

$$\Phi_{Tsh} = [\rho_{ma} - \rho_{sh}] / [\rho_{ma} - \rho_f] \quad (3)$$

$$\Phi_E = \Phi_T - (\Phi_{Tsh} * V_{sh}) \quad (4)$$

Table (1) shows the used parameters in calculating effective porosity fore upper and lower zone in raven -2well.

Zone	ρ_{ma} (gm/cc)	ρ_f (gm/cc)	ρ_{sh} (gm/cc)
Upper zone	**2.65**	**0.9**	**2.4**
lower zone	**2.65**	**0.9**	**2.4**

Table (2) shows the used parameters in calculating effective porosity fore upper and lower reservoir (Viper-Anaconda) N.Idkue -4x well

Zone	ρ_{ma} (gm/cc)	ρ_f (gm/cc)	ρ_{sh} (gm/cc)
Viper	2.63	0.9	2.11
Anaconda	2.63	0.9	2.16

4.3. Water Saturation (S_w) Calculations:

The determination of the water saturation is very important to complete the deduced petrophysical parameters of reservoir rocks

Water saturation has been calculated for Raven-2 well and N.Idkue -4x well by using resistivity log, total porosity log, shale volume log and Archie equation. Table (5.3) shows the used parameters in calculating Sw for Raven-2 well and N.Idkue -4x well.

$$Sw^{n} = R_w / \Phi^m R_t \quad (5)$$

Where S_w is water saturation, Φ -Porosity R_t – True Formation Resistivity R_w – Formation Water resistivity, n – Saturation exponent, which describes the geometry of the current flow path through the water body in the presence of hydrocarbon and m is cementation exponent

Table (3): The used parameters in calculating water saturation for upper and lower zone in Raven -2well.

zone	a	m
Upper zone	1	2
Lower zone	1	1.97

Table (4): The used parameters in calculating water saturation fore upper and lower reservoir (Viper-Anaconda) N.Idkue -4x well.

zone	a	m
Viper	1	1.98
Anaconda	1	1.96

4.4. Determination of Net Pay and Net Reservoir Thickness:

Net Pay and Net Reservoir Thicknesses have been determined by using summaries module of interactive petrophysics software, V_{sh} log, PHIT_D log, and S_w log.

Table (5): shows the used parameters calculating net pay and net reservoir thicknesses.

Well name Petrophysical parameter	Raven -2	North Idkue -4x
ShaleVolume_min (%)	**7**	**13**
ShaleVolume_max (%)	**47**	**80**
Porosity_min (%)	**10**	**25**
Porosity_max (%)	**35**	**30**
Sw_min (%)	**15**	**13**
Sw_max (%)	**40**	**80**

4.5. Lithological Identification cross-plot:

Identification of lithology is of a particular importance in formation evaluation process. Logs can be used as indicators of lithology. The most useful logs for this purpose are density, neutron, sonic and gamma-ray logs.

The following is the using of neutron vs. density and neutron vs. sonic cross-plots in all wells in the study area.

4.5.1. Qantara Formation upper Zone:

Figure (5.1) represents the neutron-density and the neutron-sonic cross-plots (lithological identification cross plot) of upper reservoir in Qantara Formation in Raven -2 well. As is shown in this figure, it is mainly characterized by the predominance of sandstone and shale but the percentage of sand higher than the proportion of shale.

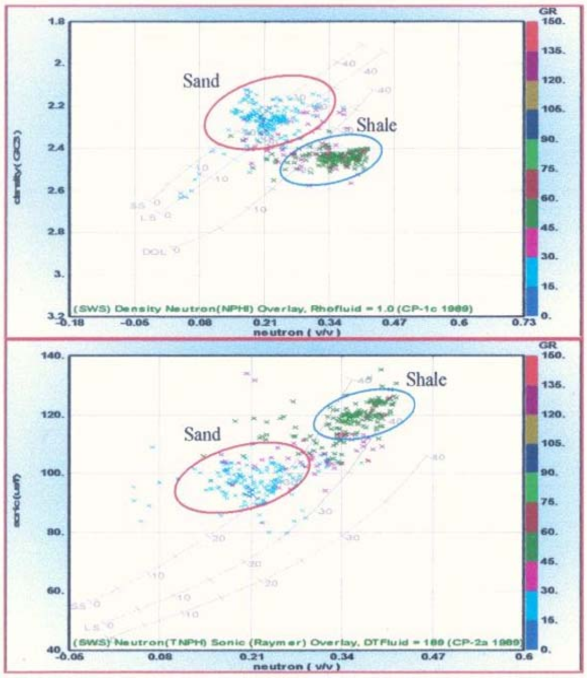

Figure (5.1): lithological identification cross-plot of upper zone member in Qantara Formation, shows the predominance of sand stone and shale.

4.5.2. Qantara Formation lower Zone:

Figure (5.2) represents the neutron-density and the neutron-sonic cross-plots (lithological identification cross plot) of upper and lower zone in Qantara Formation in Raven -2 well. As is shown in this figure, it is mainly characterized by the predominance of sandstone and shale.

4.5.3. Kafr El Sheikh Formation –upper Zone (Viper):

Figure (5.3) represents the neutron-density and the neutron-sonic cross-plots (lithological identification cross plot) of upper zone (Viper) in Kafr El sheikh Formation in one well. As is shown in this figure, it is mainly characterized by the predominance of shale and sandstone but the percentage of shale higher than the proportion of sand.

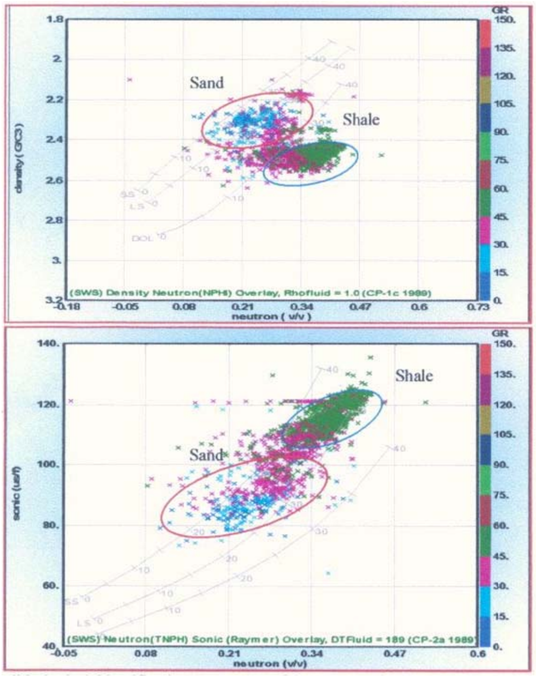

Figure (5.2): lithological identification cross-plot of lower zone in Qantara Formation, shows the predominance of sand stone and shale.

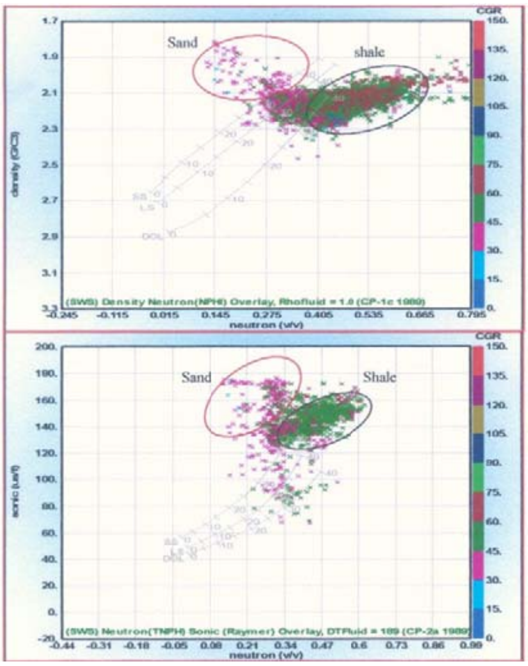

Figure (5.3): Lithological identification cross-plot of Viper channel in Kafr El sheikh Formation.showing the predominance of shale and sand stone.

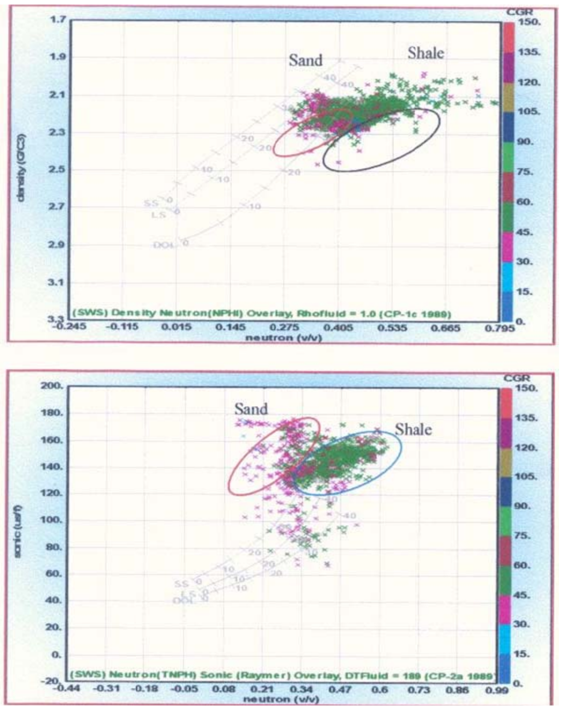

Figure (5.4): Lithological identification cross-plot of Anaconda in Kafr El Sheikh Formation.showing the predominance of shale and sand stone.

4.5.4. Kafr El Sheikh Formation –lower Zone (Anaconda):

Figure (5.4) represents the neutron-density and the neutron-sonic cross-plots (lithological identification cross plot) of lower reservoir (Anaconda) in Kafr ELSheikh Formation in one well. As is shown in this figure, it is mainly characterized by the predominance of shale and sandstone but the percentage of shale higher than the proportion of sand.

4.6.1. Litho-Saturation Cross-plot of Raven – 2 well:

Figure (6.1) represents the Litho-saturation cross-plot of upper and lower zone in Qantara Formation in Raven -2 well. As is shown in this figure the upper zone and lower zone in Qantara Formation is encountered at the depth of 4453 to 4510 m in the upper zone but from 4515 to 3807m in the lower zone. The gross interval is 57 and 292.4 in upper zone and lower zone respectively. As is shown in this figure, it is mainly characterized by the predominance of sandstone and shale. Sand stone tends to decrease in the lower zone of lower zone, where the effective porosity increases and reaches up to 25% in upper zone and 20% in lower zone the water saturation increase in upper zone reaches to 20%. In this formation as is shown in figure 69, while the water saturation increase in the lower part reaches to 35%.the shale content ranges between 7 % to 45 % but the mean value is 25 in upper zone of while in lower zone of lower zone ranges from 12% to 47% and the mean value is 22 %. The net pay is 24.08 m in upper zone of and 16m in lower zone.

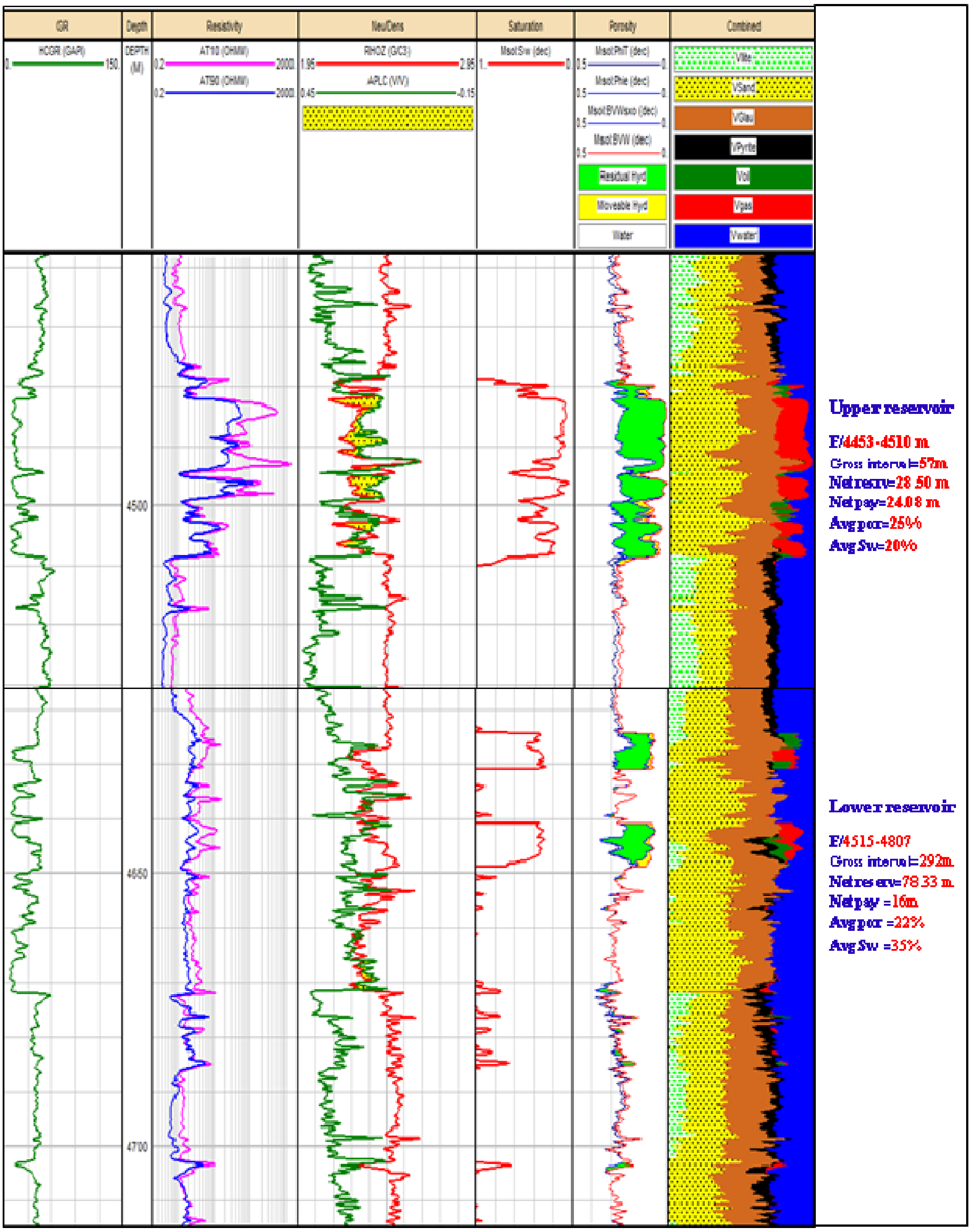

Figure (6.1): Litho-Saturation Cross-plot of upper and lower zone in Qantara Formation in Raven – 2 well.

4.6.2. Litho-Saturation Cross-plot of North Idkue – 4 well:

Figure (6.3) represents the Litho-saturation cross-plot of upper and lower reservoir (Viper and Anaconda) in Kafr ELSheikh Formation in North idkue

– 4 well. As is shown in this figure the two target in Kafr EL Sheikh Formation is encountered at the depth of 1479 to 1646 m 1916 to 2214.5 m respectively and the gross interval is 60 m and 79 in Viper and Anaconda respectively. As is shown in this figure, it is mainly characterized by the predominance of sandstone and shale. Sandstone tends to decrease and the shale increase in the lower zone of anaconda, where the effective porosity increases and reaches up to 30% in upper reservoir and 25% in lower reservoir the water saturation increase in lower reservoir zone reaches to 55%. In this formation as is shown in figure (5.12), while the water saturation decrease in the upper part reaches to 35 %.the shale content ranges between 13% to 36.1% but the mean value is 25%in upper zone of Viper while in lower reservoir of anaconda ranging from 25% to 80%.The net pay is 16 m in upper reservoir of (Viper) and 9 m in lower reservoir (Anaconda).

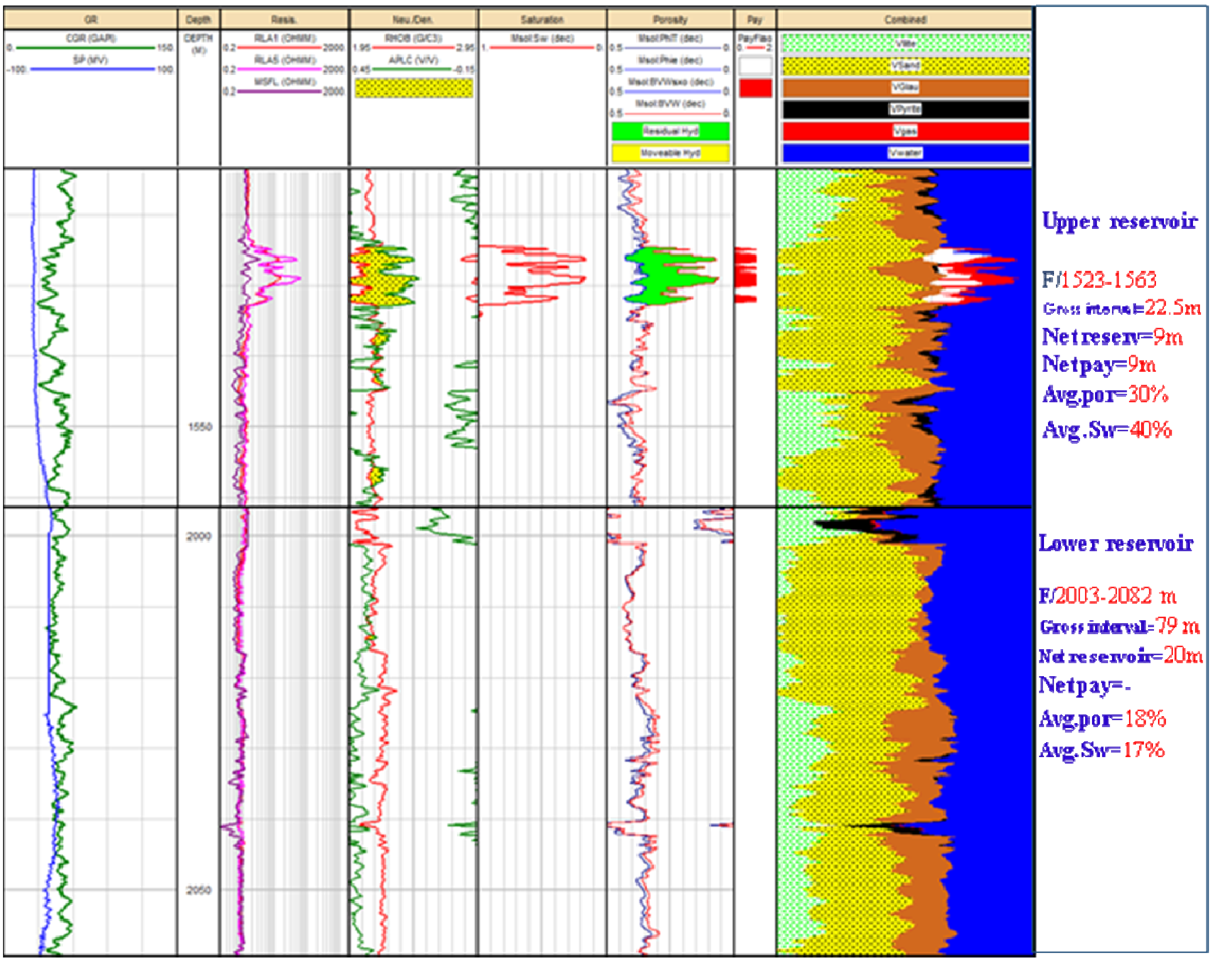

Figure (6.1): Litho-Saturation Cross-plot of upper and lower reservoir zone (Viper-Anaconda) in Kafr El sheik Formation in North Idkue – 4 well.

4.7. Seismic attributes:

The study and interpretation of seismic attributes give some qualitative information of the geometry and the physical parameters of the subsurface. In this study we used seismic attributes application (RMS amplitude, and Relative Acoustic Impedance) to delineate the channel.

4.7.2 RMS amplitude:

Amplitude varies with lithology. Anomalous seismic amplitude (e.g. bright spots) is primarily used as hydrocarbon indicators, although they can also be associated with lithology changes (Rijks and Jauffred, 1991 and Chen and Sidney, 1997). The theoretical background for seismic amplitude interpretation was already established at the beginning of last century.

According to Zoeppritz's equation the seismic amplitude dependence on seismic velocity and density in the two layer medium were analyzed. Based on these works, the equations were developed describing amplitude changes as functions of P and S wave velocities, density and angle of incidence of seismic arrival on the reflector (Zoeppritz,1919).

When we apply RMS amplitude on upper and lower channel at top of 4280msec and 4600msec figure (4.16) we shows that these channels appears high amplitude. The amplitude values at the two channels range from 3500 to 9000 and the color from gray to red. Also the RMS amplitude values at time 1700 ms and 2250ms (Viper and Anaconda channels)is very high ranging from 300 to 7000 (red to gray color) correlated to low amplitude in surrounding channel,, this value gives indication on sand channel and the hydrocarbon founded..

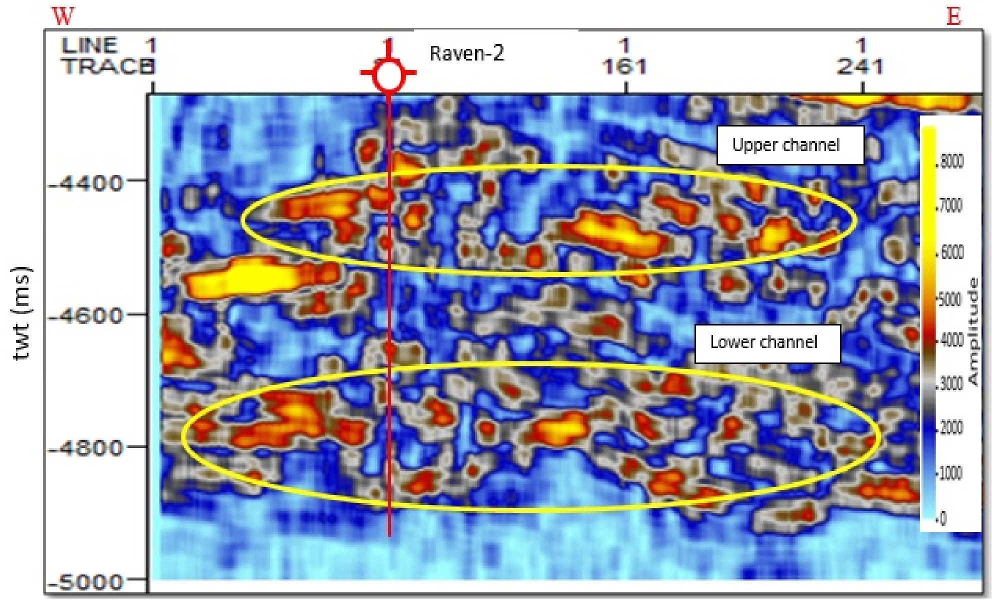

Figure (6.2): Showing the amplitude map, the two channels take trend of higher amplitude relatively to surrounding events.

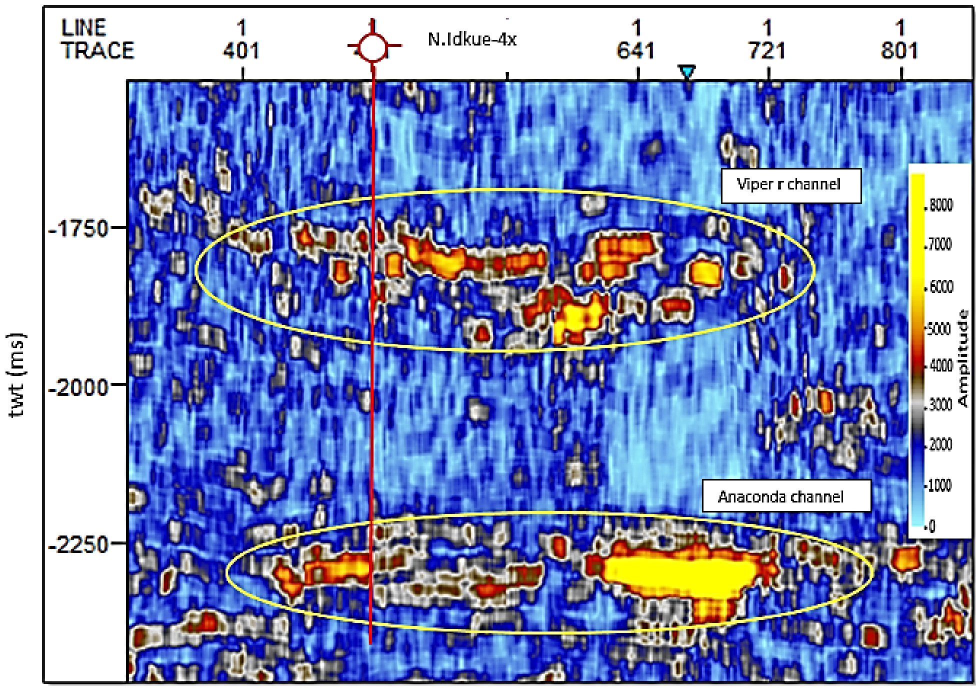

Figure (6.3): showing Root mean square amplitude applied on (Viper and Anaconda) sand channel.

4.7.3. Relative Acoustic impedance:

The Relative Acoustic Impedance (RAI) is a simplified inversion (Cobbold and Richard, 2007).

Which $$f(t) = \frac{1}{2}\Delta ln(\rho v) \quad (6)$$

$$f(t) = \frac{1}{2}\frac{\Delta\rho v}{\rho v} \quad (7)$$

Therefore, by integrating the zero phase trace, we will get the band-limited estimate of the natural log of the acoustic impedance. Since it is band limited, the impedance will not have absolute magnitudes and the stack section is usually the estimate of zero offset reflectivity; hence it is called relative acoustic impedance.

$$ln(\rho v) - 2.\int_{t=0}^{t=T} f(T)dt \quad (8)$$

The acoustic impedance values at the two channels in figure (6.4) are very low compared with

RMS amplitude at the same locations. The acoustic impedance values at upper and lower sand channels range from -5000 to 9000(green to red color).

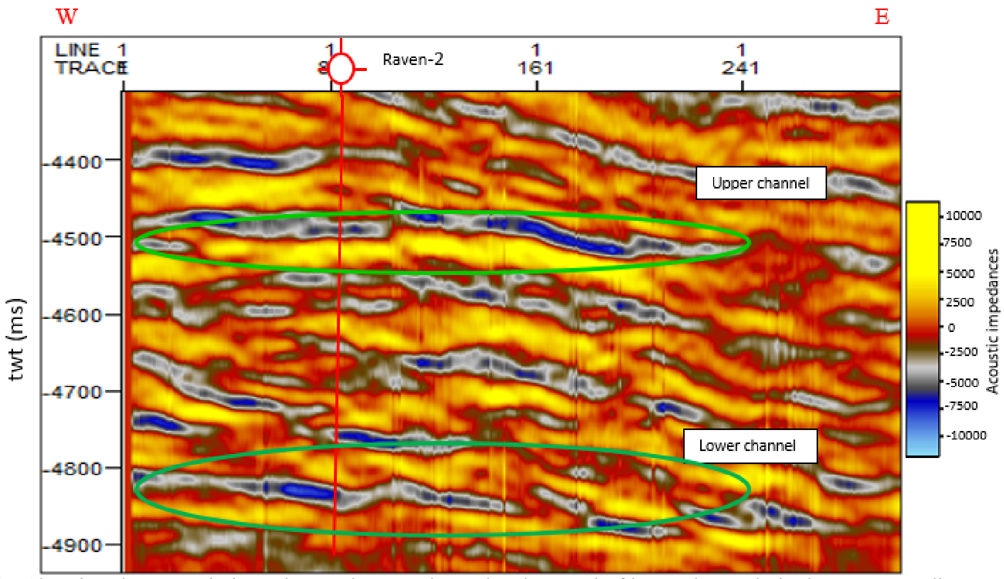

Figure (6.4): Showing the acoustic impedance, the two channels take trend of low values relatively to surrounding events.

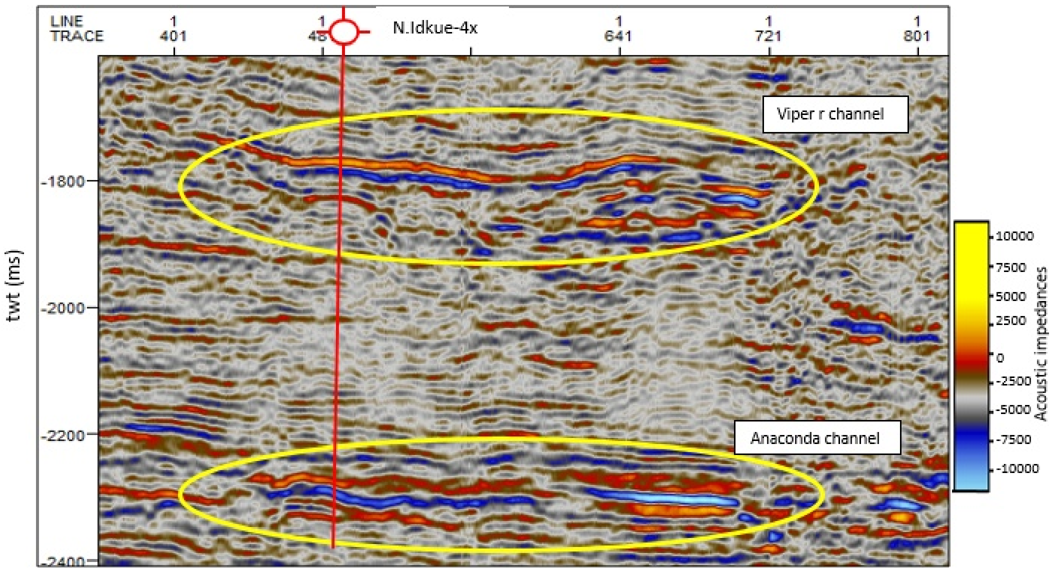

Figure (6.5): Relative acoustic impedance at 1700ms and 2250ms is low values reach to -4500 relative to surrounding events reach to 7000 and the channel take E-W trend.

But the host rock is a high values ›4500 (violet color).where the Relative acoustic impedance at time 1700msec and 2250ms figure (6.5) (viper channel and Anaconda) is low value <-7500. The acoustic impedance variation within the channel complex may be correlated to sand/shale ratios. Higher values of Relative acoustic impedance (RAI) seem to be related to shale intervals inside the body of the channel (green color)

Conclusion:

The present study aimed to analyses the well log data of the gas-bearing sand anomalies of the Pliocene and lower Miocene sediments of Kafr El Sheikh and Qantara Formation in the off-shore Nile Delta area (North Maryut concession). Complete petrophysical analysis is performed over two wells (Raven -2 and North Idkue -4x) scattered in the study area. Such analysis reveals the presence of four gas-bearing sand anomalies (Viper and Anaconda zone in Kafr El Sheikh Formation and the upper and lower zone in Qantara formation).The log characteristic of the hydrocarbon of the four gas-bearing sand anomalies are showing that the high resistivity, high porosity and low gamma ray. According to seismic amplitude and acoustic impedance that applied on the four anomalies in Qantara and Kafr ELSheikh us showing that the four anomalies appear a high amplitude and low acoustic impedance, this indicator on sand bearing gas.

Acknowledgments:

The authors thank the Egyptian General Petroleum Corporation (EGPC).

Reference:

1. Abdel Aal, A.; El Barkooky, A.; Gerrits, A.; Meyer, H.; Schwander, M.; Zaki, H.(2000): Tectonic evolution of the Eastern Mediterranean Basin and its significance for hydrocarbon prospectivity in the ultra-Deepwater of the Nile Delta. The Leading Edge, p. 1086-1102.
2. Asquith, G., and D. Krygowski, 2004: Basic Well Log Analysis. American Association of Petroleum Geologist, pp. 244. The Colony and Sparky members of the Mannville Group are currently producing oil in the area, and are the main exploration targets of the survey.
3. Chen, Q., AND Sidney, S., (1997): Seismic attribute technology for reservoir forecasting and monitoring: The Leading Edge, v.6, p.445-448.
4. Cobbold, S.C. Richard, 2007: Foundations of Biomedical Ultrasound. New York: Oxford University Press. Pp: 41-42.
5. Dolson J., Shann M., HammoudaH, RashedR, and MatboulyS: The Petroleum potential of Egypt, Petroleum Provinces of the 21st Century, San Diego, California, 2000.
6. Eni/Agip, Gepe-Espr (June 2000): Egypt – Offshore Nile Delta Integrated Regional Study, Approved by Proj. Manager: San Donato Mil, P.9-80.
7. Hemdan S. and Jonathan M: Nile Delta Gas Origin and Biogenic Gas Potential.
8. Meshref, W.M., 1982: Regional Structural Setting of Northern Egypt.Proceedings of the 6th exploration seminar, EGPC, Cario, pp: 17-34.
9. Nini C., Checchi F., El BlasyA.andTalaat A: Depositional evolution of the Plio-Pleistocene succession as a key for unraveling the exploration potential of the post-Messinian play in the Central Nile Delta, MOC2010.
10. Rijks, E.J.H., and Jauffred, J.C.E.M., (1991): Attribute extraction: An important application in any detailed 3D interpretation study: The Leading Edge, v.10, p.11-19.
11. Tawadros E: Geology of Egypt and Libya, BalkemaA. p. 146-155, 2001.
12. Schlumberger, (1972): Log interpretation, Volume I – Principles.
13. Shuey, H., (1985): A simplification of the Zoeppritz equations. Geophysics 50, pp. 609–614.
14. Zoeppritz, K. (1919): On the reflection and propagation of seismic waves at discontinuities, Erdbebenwellen VIIB, Goettinger Nachrichten I, pp. 66–84.

11/28/2014